Future Cities and Environment
ISSN 2363-9075 Volume 11 (2025)

https://doi.org/10.70917/fce-2025-030
Article

Multi-Level Simulation for Dynamic Analysis of A Domestic Electric oven in Forced Convective Heating—Evaluation and Optimization of Energy Consumption Using the Brick Test

Simona Rustico [1,*], Beatrice Pulvrenti [1], Giorgia Useli [2] and Marco Reguzzoni [2]

[1] Department of Industrial Engineering, University of Bologna, Viale Risorgimento 2, 40136 Bologna, Italy; beatrice.pulvirenti@unibo.it
[2] R&D Department, SMEG s.r.l, Via Leonardo da Vinci 4, 42016 Guastalla (RE), Italy; giorgia.useli@smeg.it (G.U.); marco.reguzzoni@smeg.it (M.R.)
* Corresponding author: simona.rustico2@unibo.it

Abstract: The study proposes a novel method aimed at the optimization of the energy consumption of a domestic electric oven. The goal is to achieve the best trade-off between the oven energy consumption and its performance in terms of thermal distribution. The method revolves around a multi-level analysis that couples detailed, steady-state CFD results with the transient evaluation of the associated lumped parameters. In particular, the distribution of the heat transfer coefficients (convective and radiative) is computed through the CFD analysis and used as the input for the dynamic analysis to get the time evolution of the oven energy consumption. The tested oven has a volume of 68L and is equipped with three heating elements. The numerical model has been validated through measurement data on the temperature distribution, showing high accuracy in predicting the thermal behaviour and energy fluxes of the cavity. Moreover, experimental validation of the energy consumption has been performed following the EN 60350 standard, which involves a wet brick initially cooled to 5 ± 2 °C and then heated until its core temperature rises by 55 °C. Results suggest that this approach can lead to a substantial reduction of the oven energy consumption while maintaining high performance standards.

Keywords: oven; energy consumption; CFD

1. Introduction

In recent years, standards such as EN 60350 (CENELEC 2013) have become increasingly stringent, raising energy efficiency requirements for household electric cooking appliances. This evolution is motivated by the significant environmental impact of such systems. In fact, these appliances account for approximately 25% of the overall environmental impact of buildings. Electric ovens play a central role in this, particularly in apartment settings (Hoxha, 2017). Moreover, the ovens are among the least energy-efficient domestic appliances, with typical efficiencies ranging between 10% and 12% (Amienyo, 2016), thereby motivating the development of more efficient technologies to reduce energy consumption (Bansal, 2011).

Most of the recent innovations focus on the improvement of the control strategies. The approaches rely either on temperature prediction methods defined by current regulations or on structural modifications of the appliances themselves. However, limited attention has been given to the direct control and optimization of electric heating elements. In this context, the present study introduces a novel stepwise control strategy aimed at improving energy efficiency through enhanced heating elements

management.

Several numerical studies in the literature have addressed the transient thermal behavior of domestic ovens. Verboven et al. (Verboven,2000) developed a three-dimensional CFD model for heat transfer in a forced convection oven. In their approach, radiation effects were included indirectly via externally calculated boundary conditions, a method that compromises quantitative accuracy. Mistry et al. (Mistry, 2006) extended this modeling by incorporating radiative effects directly, analyzing transient natural convection during baking and broiling cycles using a CFD framework.

While CFD analyses provide detailed thermal insights, they are not suited for control design due to their computational intensity. For this reason, low-order models based on lumped parameter methods are widely adopted for system-level thermal analysis and control applications. In this context, Laboreo et al. (Laboreo, 2014, Laboreo, 2016) developed a dynamic model of a domestic oven using electrical analogies and lumped parameters. They include the thermal dynamics of a load subject to water evaporation during convection and radiation cooking.

Other studies have explored simplified but effective modeling strategies. Burlon et al. (Burlon,2017) presented a lumped model excluding thermal load. The radiative exchange was modeled without linearization, and convection coefficients were calibrated as tunable parameters. Lucchi et al. (Lucchi, 2019) proposed a lumped model simulating the standard brick test, using experimental power data as input. They identified thermal conductances and capacities through optimization based on measured data. The moisture evaporation was modeled by splitting the brick into internal and external regions, and linking saturation pressure to surface temperature.

Following the development of accurate thermal models, attention has shifted to improving energy efficiency. Pensek et al. (Pensek,2005) identified key factors influencing oven performance. They proposed several improvements, such as enhanced door sealing, additional insulation, and operational cycle optimization. These lead to measurable gains in energy efficiency ratings. Similarly, Sari et al. (Sari, 2013) studied the impact of different insulation configurations. They found that an optimized design can reduce energy use by up to 4.5%, as confirmed by infrared thermography.

Shaughnessy et al. (Shaughnessy, 2000) compared a low-emissivity oven prototype with a commercial unit. The energy savings were of 36–57% under standard testing conditions without compromising thermal performance. More recently, Mayil et al. (Mayil, 2022) focused on heater control, investigating multiple on-off cycling patterns to improve energy efficiency, minimize thermal losses, and stabilize internal temperatures.

Against this background, the present work proposes a two-level simulation approach to analyse the energy performance of a domestic oven. A steady-state CFD analysis was conducted using STAR-CCM+ (Siemens, Academic Power On Demand, 2024) to extract heat transfer coefficients, and a dynamic simulation model was implemented in MATLAB/Simulink (MATLAB/Simulink). The CFD data provide accurate convective and radiative parameters used as inputs in the low-order model to compute time-dependent energy behavior.

The energy-saving strategy presented in this work is based on a new control of the heating elements. The total heating time is divided into three time phases, each with configurable activation states and percentages for the grill and bottom heaters. Several configurations were simulated and compared against the oven's original control logic, demonstrating the effectiveness of the proposed method in reducing power consumption while maintaining thermal performance.

2. Methodology

2.1. Experimental Setup

The oven used for the simulation and experiments is a domestic electric model with an internal cavity volume of 68 cm^3. This model has three heaters: two top heaters of 1700W and 1000W, and one bottom heater of 1200W, located in a drawer below the cavity. An upper heater and a lower heater have an undulating closed-loop shape. The other upper heater is rectangular and extends closer to the walls.

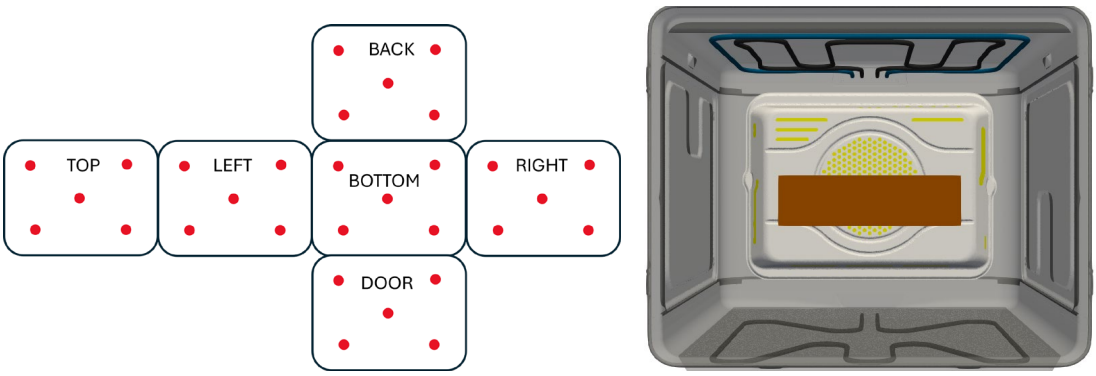

a) b)

Figure 1. Experimental setup. (**a**) Placement of thermocouples on each internal surface of the oven cavity, including the glass door, used for temperature monitoring during tests. (**b**) Interior view of the oven showing the positioning of the heating elements and the wet brick at the center, as required by the EN 60350 standard test.

The first phase of the experimental procedure focused on temperature measurements within the oven cavity and on its internal surfaces. The T-type thermocouples used in the experiments were previously calibrated using a certified temperature calibration bath and verified against a precision Pt100 reference sensor. Calibration was performed in the temperature range relevant to the study (20–200°C), ensuring a measurement uncertainty within ±0.5°C. Their placement on the walls and within the cavity is detailed below:

- Five thermocouples for each oven wall, including the glass door. Figure 1a) describes the placement of the thermocouples for each wall.
- One thermocouple placed in the oven center (OC).
- One thermocouple to record ambient air temperature.

Temperature data from the wall sensors were averaged to obtain representative values for each surface. Additionally, a Pt1000 temperature detector was installed inside the cavity to provide input to the oven's heating control logic (on-off regulation).
Power consumption was monitored using a precision wattmeter with an accuracy of ±0.1%. All tests were conducted in an air-conditioned environment at a controlled ambient temperature of 21 ± 2°C.

In the second phase of the procedure, a standardized energy consumption test was performed. The test followed the EN 60350 standard (CENELEC, 2013) and was conducted at SMEG laboratories using the same oven model and convection heating function. The test procedure involves heating a wet brick, initially cooled to a uniform temperature of 5 ± 0.5°C, as monitored by two embedded thermocouples.

The brick is placed at the oven cavity's center (see Figure 1b). During the test, the oven's power consumption and the on-off cycles of the sensor were recorded. At the end of the test, the two basic parameters for the oven's energy efficiency are recorded: total duration and energy consumption.

2.2. CFD Analysis

The commercial software STARCCM+ has been used to perform the CFD analysis. The analysed governing equations consist of mass (1), momentum (2), and energy (3) balance equations for steady-state, incompressible, turbulent flows of an ideal gas, namely:

$$\nabla \cdot \vec{v} = 0 \tag{1}$$

$$\rho_0\left[\left(\vec{v}\cdot\vec{\nabla}\right)\vec{v}\right] = -\nabla(\mathrm{p} + \rho_0 g z) + \rho_0 g\beta(T - T_0)\nabla\mathrm{z} + \vec{\nabla}\cdot\tilde{\tau}_{eff} \tag{2}$$

$$\vec{\nabla}\cdot\left(\vec{v}(\rho e + p)\right) = \vec{\nabla}\cdot[(k + k_t)\nabla\mathrm{T} + \tilde{\tau}_{eff}\cdot\vec{v}] \tag{3}$$

where $\vec{v}$ is the velocity vector, p is the pressure, β is the thermal expansion coefficient, $\tilde{\tau}_{eff}$ is the effective stress tensor, e is the specific enthalpy, k is the thermal conductivity and k_t the turbulent thermal conductivity.

The Reynolds Stress Transport (RST) turbulence model and the Elliptic Blending near-wall Reynolds-stress turbulence closure were utilized. This model better accounts for turbulence anisotropy (Lardeau, 2014). The governing equations were discretized into a set of algebraic equations using a

second-order upwind scheme, and the pressure-velocity coupling problem was solved using the semi-implicit method for pressure-linked equations (SIMPLE algorithm). The simulation was monitored for convergence by measuring residuals, velocity, and temperature values at various randomly selected points in the cavity. The mesh consisted of 12×10^6 elements with a base size of 6 mm. A boundary layer was modelled with 5 layers and a total thickness of 5% of the base size. Additionally, surface refinements were necessary for the heating elements, and the vents placed in the baffle were used to recirculate air inside the cavity. The details about the mesh refinement are shown in Figure 2.

The simulation was performed in steady-state with a set-point temperature of 190°C and reproduced the static mode. The two heating elements turned on were modeled as heat sources, obtaining a temperature of 300 °C. A rotating region around the fan was created in the software simulation to simulate the fan's rotation. The walls are modelled as convection with 1,718 W/m^{2}K. The brick also has a convection condition with a value of 12 W/m^{2}K for the back faces, 15 W/m^{2}K for the bottom face and 2 W/m^{2}K for the other faces.

The radiation heat transfer was considered by applying the surface-to-surface radiation model (Siegel, 1992). In this model, the air is considered a transparent medium, and all surfaces are assumed to be diffusive and grey. To solve the surface-to-surface (S2S) radiative model, equations describing the radiation flow between surfaces are required. These equations can be based on the Stefan-Boltzmann law, which relates the radiation emitted by a surface to its temperature, area, and optical properties. The energy reflected from the generic surface K can be written as:

$$q_{out,K} = \varepsilon_k \sigma T^4 + \rho_K q_{in,K} \tag{4}$$

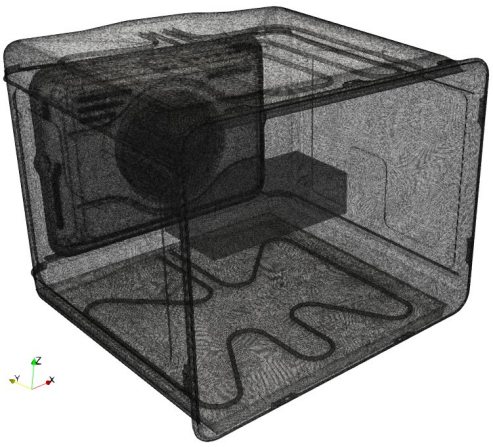

a)

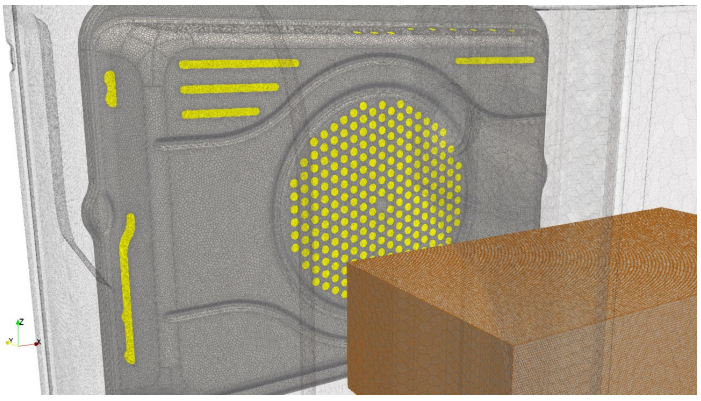

b)

Figure 2. Computational mesh used in the CFD simulation. (**a**) Full view of the mesh applied to the oven cavity. (**b**) Refined mesh details for critical regions, including the wet brick, baffle, and air vents, to ensure accurate resolution of thermal and flow gradients.

2.3. Dynamic Analysis

The dynamic model was developed using the Simscape language in the MATLAB/Simulink environment. Simscape makes it possible to create models of physical components based on physical connections directly integrated with block diagrams. These tools use local equations associated with each element to describe the physical behavior of the system.
The dynamic model was structured into three main blocks:

- A block for evaluating the heat transfer between the walls, between the air in the cavity and the walls, and between the walls and the external environment. This block includes all the equations describing the heat exchanges, modeled according to conduction, convection and radiation laws.
- A block for the heating elements control implements a control system based on hybrid on/off logic combined with a PID logic to drive the activation of heating elements to reach the target temperature.
- A block to display energy consumption calculates and displays the oven's energy consumption in real-time, indicating the system's energy performance.

Figure 3 shows the model with the three blocks. There is also a knob used to set the desired temperature inside the oven and a scope for displaying temperatures. This modular breakdown enables the precise organization of the model, facilitating its analysis and modification.

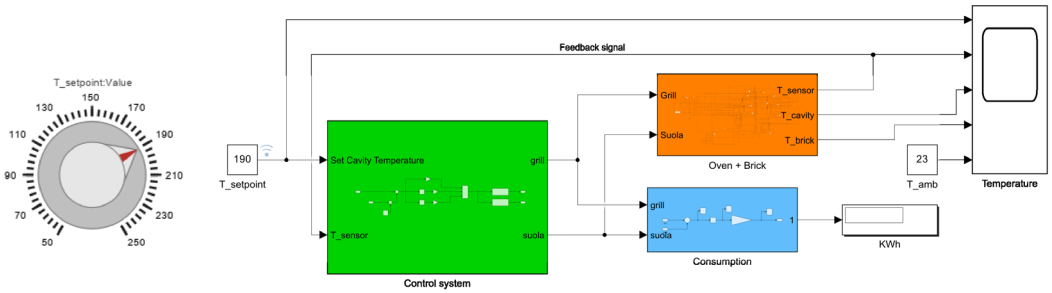

Figure 3. Simulink implementation of the dynamic oven model. The simulation consists of three core modules: the heater controller (green), the physical model of the oven and brick (orange), and the energy consumption monitor (blue). A user-defined setpoint knob and a temperature display scope are included for control and visualization during runtime.

2.4. Lumped Parameters Model

The oven cavity has been subdivided into seven parts: bottom (BW), right (RW), left (LW), back (BaW), top (TW), the glass door (DW) and the air inside the cavity (OC). In the actual oven, a Pt1000 temperature sensor is installed in the upper-left corner to monitor the transient thermal response. This sensor is also incorporated into the model, as it provides the sole temperature feedback during operation. Additionally, two elements simulating the thermal behavior of the heating elements are included: the bottom heater (BH) and the top heater (GH). In the lumped parameter model, each wall, heater, and the sensor is represented as a distinct node. The evolution of the temperature T_j at a generic j is governed by a non-linear differential equation, given in Equation 6. In this equation, the term $\dot{Q}_{ij}$ represents the conductive heat transfer between the nodes i and j, modeled as $G_{ij} = (T_i - T_j)$. The term G_{ij} is the thermal conductance between nodes i and j. Conductances values are reciprocal, i.e. $G_{ij} = G_{ji}$. The net heat flow into a node alters its internal energy, which is directly proportional to its thermal capacitance C_i. Additionally, the radiative heat exchange between nodes i and j, denoted $\dot{Q}_{ij}^{rad}$ is expressed as:

$$\dot{Q}_{ij}^{rad} = G_{ij}^{rad}\sigma\,(T_i^4 - T_j^4) \tag{5}$$

Here, G_{ij}^{rad} is the radiative thermal conductance, σ\sigmaσ is the Stefan–Boltzmann constant, and temperatures T_i and T_j are expressed in Kelvin. Radiative conductances also satisfy the reciprocity condition: $G_{ij}^{rad} = G_{ji}^{rad}$.

The general governing equation becomes:

$$C_j \frac{dT_j}{dt} = \dot{Q}_{\iota J} + \dot{Q}_{IJ}^{rad} + P_{el,i} \quad (6)$$

where $P_{el,i}$ represents any external power input from heating elements (Lucchi, 2019). Radiation is identified as the dominant heat transfer mechanism within the cavity, primarily due to the high temperatures of the heating elements. Despite the use of low-emissivity coatings on the oven walls and door to reduce heat losses. Significant thermal gradients, especially during transient phases or when the top heater is active, result in considerable radiative fluxes that shape the cavity's thermal dynamics.

To quantify this, a simplified estimation was performed based on experimental data for a set-point temperature T_{set} = 190 °C. Under steady-state conditions, the top heater reaches T_{TH} = 300 °C, while representative cavity temperatures are: T_{BW} = 220 °C, T_D = 160°C, and approximately of 190 °C for the other walls (RW, LW, BaW, TW). Radiative heat exchanges were computed using manufacturer-provided emissivity values: ε_{walls}=0.8, ε_{glass_door}=0.23 and ε_{heater}=0.75. View factors were determined via a MATLAB® script by Lauzier, employing the Contour Double Integral Formula (CDIF) to compute the exchange between planar surfaces (Lauzier). The top heater was modeled as a planar surface visible to all oven walls. Radiative interaction between the bottom wall and the top heating elements was neglected, as their inclusion led to an overestimation of T_{BW}, reducing the accuracy of central cavity temperature predictions.

The convective and radiative coefficients, obtained from CFD simulations in steady-state conditions, were integrated into the model to enhance the fidelity of internal heat exchange representation.

In accordance with the EN 60350 (CENELEC, 2013) standard, oven performance is evaluated under standardized conditions. The test involves placing a water-saturated brick, initially cooled to 5 °C, at the center of the oven. Two thermocouples embedded within the brick monitor its temperature evolution throughout the test, providing a consistent method for measuring energy consumption.
During the energy consumption test, the brick undergoes a process consisting of a combination of four main mechanisms:

- Transient thermal diffusion.
- Water diffusion through a porous medium.
- Water evaporation at the outer surface due to the hot air flowing around the brick.
- Water drip.

The last term can be considered negligible for simplicity, while the water and thermal diffusion terms are modeled with a lumped parameter approach. In particular, the brick is defined by two nodes, one associated with the external part and one associated with the internal part of the brick (Lucchi, 2019).

2.5. Modeling of Heating Elements On-Off Logic

The term $P_{el,i}$ in Eq. (6) represents a heat source term and is non-zero only for the nodes corresponding to the heating elements, in those two nodes its value may vary in time assuming zero value when the heating element is turned off.

$P_{el,i}$ is an input value and is intended to model the complex logic that is behind the temperature regulation of a household oven. During the initial heating phase where $T_{OC} < T_{set}$ each active heating element operates at its nominal power $P_{norm,i}$.

Once the setpoint is reached, the system transitions to a maintenance phase, where the elements are modulated using an on-off duty cycle to maintain the temperature near the desired value.
A Proportional-Integral-Derivative (PID) controller is implemented to regulate the switching behavior of the heating elements. The control signal $f(t)$ is defined as:

$$f(t) = k_p e(t) + k_I \int_0^t e(t)\, d\tau + k_D \frac{de(t)}{dt} \quad (7)$$

where $e(t) = T_{set} - T_{sensor}$ is the control error, defined as the difference between the desired setpoint and the actual cavity temperature measured by the Pt1000 sensor. The proportional term $k_p e(t)$ provides an immediate corrective action based on the magnitude of the error, while the derivative term $k_D \frac{de(t)}{dt}$ anticipates system response by reacting to the rate of change of the error.

The integral term is disregarded in this application, as it accumulates residual errors over time, an undesirable behavior in systems with slow thermal dynamics, such as domestic ovens. This simplification avoids overshooting and improves system stability during steady-state operation (Åström,1995).

The control logic allows flexible adjustment of the heater activation profile by modulating the duty cycle. This feature is critical to implementing the proposed multi-step energy-saving strategy. The

strategy divides the total cooking period into three phases, each with a distinct heating element activation percentage. This time-division strategy reduces power consumption while maintaining satisfactory thermal performance.

The proposed modeling approach offers a practical trade-off between physical accuracy and computational efficiency. By extracting thermal coefficients from steady-state CFD analysis and incorporating them into a low-order dynamic model. The method allows fast simulation of the oven's thermal behavior without sacrificing key physical phenomena. Unlike full CFD-based strategies, which are often impractical for control applications due to their computational cost, this hybrid framework is well-suited for control-oriented analysis and real-time strategy development. Its modularity also facilitates adaptation to different oven geometries and operating conditions.

3. Energy Analysis

The control strategy and thermal model having been established, we now turn to a detailed analysis of energy behavior within the oven system. This includes evaluating heat losses and the discussion of the proposed optimization method.

3.1. Heat Losses

The dynamic model enables a detailed analysis of heat losses within the oven. Figure 4 (A) shows the distribution of convective losses from each internal surface and the heating elements. The grill heater results in the highest losses. This is due to its elevated temperature and its position at the top of the cavity.

Despite being located outside the cavity, the bottom heater also contributes significantly to heat loss. This occurs through the lower drawer, where thermal insulation is less effective. The oven door accounts for 11.45% of total losses. Although made of low-emissivity glass, its large surface area and exposure to the ambient environment increase heat dissipation.

The bottom wall shows a loss contribution of 17.41%. This is attributed to the insulation being different from the other walls. The back wall has the lowest losses due to its better insulation and reduced exposure to direct heat flow. Side and top walls also show limited losses thanks to their effective insulation and less exposure.

Figure 4 (B) illustrates radiation losses. The bottom heater again shows the highest contribution, mainly due to its high temperature and placement below the cavity. The grill is the second main contributor, consistent with its radiative output and cavity location. The door and bottom wall also show notable radiation losses, confirming trends seen in convection. Other walls exhibit negligible radiation losses.

This analysis helps identify critical components where energy is wasted. It is essential for developing targeted strategies to reduce overall energy consumption.

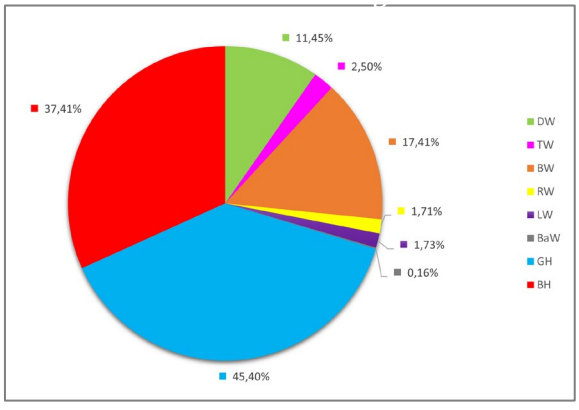

(A)

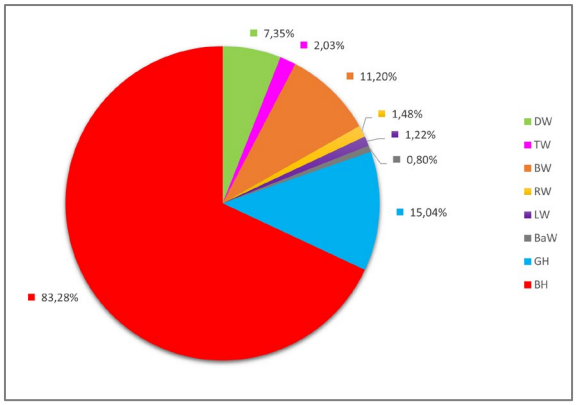

(B)

Figure 4. Distribution of heat losses within the oven cavity for convection (**A**) and radiation (**B**). The contribution of each wall and active heating element (Grill Heater – GH, and Bottom Heater – BH) is shown. The grill heater exhibits the highest convective losses, while the bottom heater dominates in radiative heat loss due to its placement and operating temperature.

3.2. Optimization Efficiency

The heat loss analysis highlighted the grill and bottom heaters as the main sources of energy inefficiency. Their high operating temperatures and specific positions in the oven cavity contribute significantly to both convective and radiative losses.

Improving oven energy efficiency typically involves structural modifications. These include better insulation, improved door sealing, or design changes. While effective, such solutions are costly and time-consuming to implement.

To offer a more practical alternative, a control-based strategy was developed. The method divides the heating cycle into three time steps. Each step is characterized by specific parameters that define heater activation percentages and optional fan operation. A temperature offset can also be applied to correct for thermal losses or adjust for specific cooking requirements.

The heating elements (GH and BH) are modulated using a duty cycle approach. Specifically, a 50% activation means the element is on for half of the control interval and off for the other half. In this study, the fan remains constantly active during all steps to maintain forced convection. The offset value is kept constant across the entire cycle.

This strategy allows precise control of energy input, reducing unnecessary power usage while preserving thermal performance. It offers a flexible and low-cost solution for optimizing energy consumption in domestic ovens.

4. Results

The proposed control strategy was tested through both simulations and experiments. In the following section, we present the results of these validations, focusing on model accuracy, thermal field distributions, and energy savings.

4.1. Validation at Tset = 190 °C

The test for model validation was conducted with a cavity setpoint temperature of 190 °C. Figure 5 (a) compares the temperature profiles over time obtained from both experimental measurements (blue) and model predictions (orange) for each wall and at the cavity center.

The agreement between the model and the experimental data is strong. The average error remains below 2% for the entire duration of the simulation, confirming the model's accuracy in capturing transient thermal behavior.

Figure 5 (b) shows the temperature comparison for the Pt1000 probe and the brick core. In both cases, the model closely follows the measured data, demonstrating that the thermal dynamics of both the air and the thermal load are reliably reproduced.

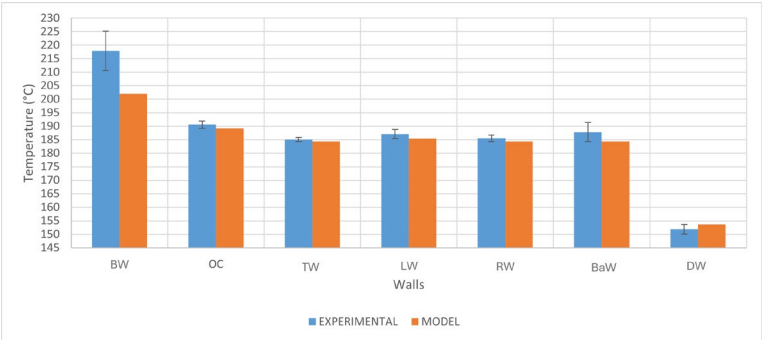

(a)

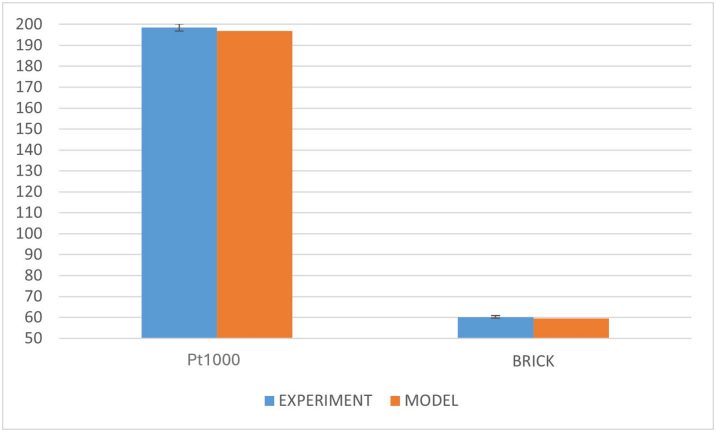

(b)

Figure 5. Validation of the dynamic model through temperature comparison. (**a**) Simulated versus experimental temperatures at various oven surfaces and the cavity center. (**b**) Comparison between simulated and measured temperatures from the Pt1000 sensor and the core of the wet brick during the energy test at 190 °C.

4.2. CFD Results

Figures 6 and 7 illustrate the temperature and velocity distributions within the oven cavity, obtained from CFD simulations under steady-state conditions.

The temperature field in Figure 6 exhibits significant non-uniformity, especially near the heating elements. As expected, lower temperatures are observed in the door region, while higher temperatures are concentrated near the grill and bottom heaters.

The velocity field in Figure 7 confirms the influence of the fan and internal geometry on airflow distribution. Two primary recirculation zones are visible: one directed towards the lower-left side, and the other towards the upper-right section. The presence of the brick modifies airflow patterns locally, as it obstructs part of the central cavity space.

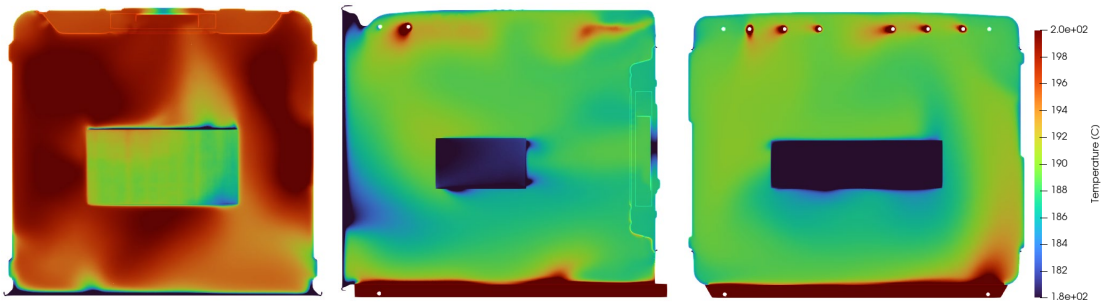

(a) (b) (c)

Figure 6. CFD-simulated temperature distribution across three orthogonal cross-sections of the oven cavity. (**a**) plane normal to z-axis; (**b**) plane normal to x-axis; (**c**) plane normal to y-axis. High temperature gradients are observed near the grill and bottom heaters, while the door region shows significantly lower temperatures.

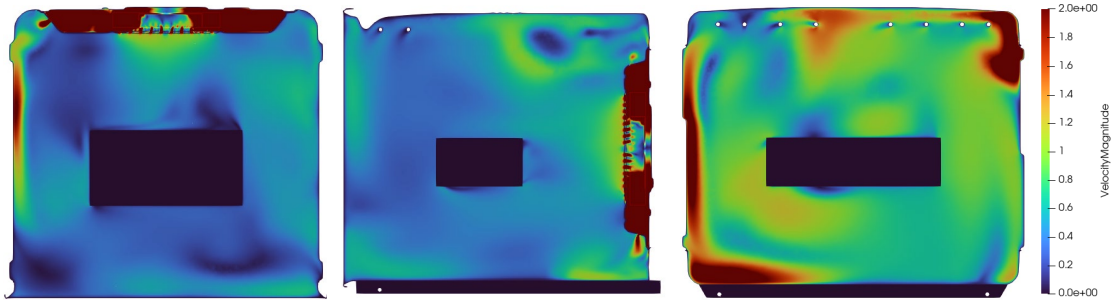

(a) (b) (c)

Figure 7. CFD velocity magnitude distribution within the oven cavity. (**a**) plane normal to z-axis; (**b**) plane normal to x-axis; (**c**) plane normal to y-axis. Recirculation flows generated by the fan are evident, particularly along the lower-left and upper-right zones. Airflow is locally disturbed by the presence of the thermal load (brick).

4.3. Optimization Efficiency Results

To assess the effectiveness of the implemented control strategy, we conducted a detailed analysis of energy efficiency improvements under various heating element activation scenarios. Table 1 presents the results of five cases, each with different heating element activation percentages. Energy consumption is reported in kilowatt-hours (kWh), along with the corresponding percentage savings and model prediction error.

***Table* 1.** Case studies for the consumption test.

CASES	GH (W)	BH (W)	Consumption (kWh)	Saving (%)	Error (%)
Case 0	$P_{nom,GH}$	$P_{nom,BH}$	1.039	0	± 3
Case 1	$P_{nom,GH}$ * 0.95	$P_{nom,BH}$ * 0.6	1.012	2.6	± 3
Case 2	$P_{nom,GH}$ * 0.9	$P_{nom,BH}$ * 0.5	0.994	4.33	± 3
Case 3	$P_{nom,GH}$ * 0.85	$P_{nom,BH}$ * 0.4	0.988	4.91	± 3
Case 4	$P_{nom,GH}$ * 0.8	$P_{nom,BH}$ * 0.1	0.913	12.3	± 3

Case 0 represents the baseline condition, with both heating elements operating at full nominal power. In subsequent cases, the grill and bottom heater power levels are progressively reduced.

The results show a clear trend: decreasing the activation percentage of the heating elements leads to

lower energy consumption. In Case 4, with the bottom heater reduced to just 10% of its nominal power, energy savings reach 12.3% compared to the baseline. Importantly, all cases maintained the same thermal performance, with the brick reaching the target core temperature in each test.
The strategy confirms that intelligent modulation of heater activation can reduce energy demand without compromising cooking outcomes.

5. Discussion

The results obtained allow for a broader evaluation of the method's effectiveness and its implications. In this section, we interpret the findings in the context of existing literature and practical applications.

The comparative analysis of the five proposed control strategies for heating element modulation demonstrates a clear relationship between energy savings and the reduction of heater activation time. While maintaining a constant set-point temperature of 190 °C throughout all simulations and experimental tests, the brick consistently reached the target core temperature, confirming that thermal performance was preserved despite the energy-saving interventions. Figure 8 summarizes the relative savings for each case. The results highlight that a progressive reduction in the power supplied to the heating elements, especially the bottom heater, leads to significant improvements in energy efficiency. Case 4, with a 90% reduction in the bottom heater's activation rate, achieved the highest energy savings (12.3%) without compromising the thermal dynamics of the oven. This suggests that the bottom heater plays a disproportionate role in total energy consumption and that its contribution can be optimized through targeted control rather than full-time activation.

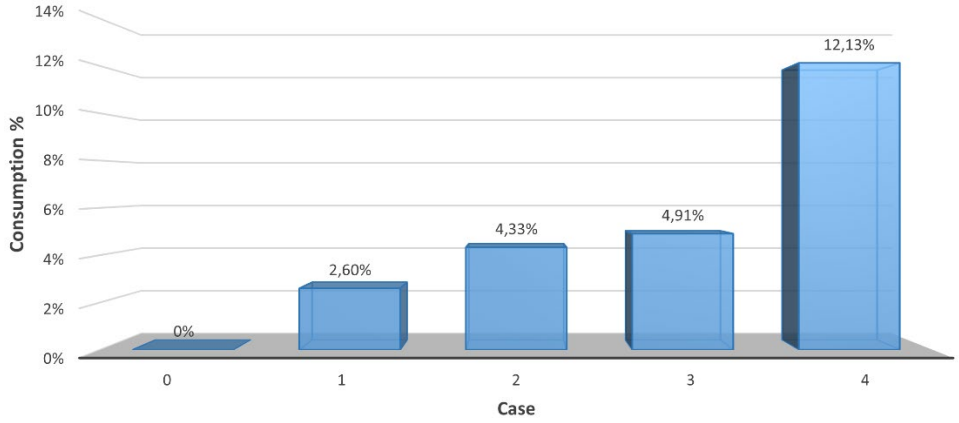

Figure 8. Relative reduction in energy consumption for five control strategies with varying heater activation percentages. The x-axis indicates each test case; the y-axis shows the corresponding percentage savings compared to the baseline (Case 0). Maximum savings of 12.3% are achieved in Case 4 with minimal bottom heater usage.

The heat loss analysis provided deeper insight into the distribution of inefficiencies within the oven. Both convection and radiation losses were highest for the bottom and grill heaters, primarily due to their location and high operating temperatures. This allowed us to focus on a method aimed at optimal heating element management. Compared to traditional energy-saving approaches, which often involve expensive and time-consuming modifications such as improved insulation or component redesign, the proposed control logic offers a flexible and low-cost solution. The modular structure of the dynamic model facilitates adaptation to ovens with different cavity geometries or insulation configurations, thus expanding its applicability. Beyond performance improvements, the modeling framework itself represents a methodological advancement. The integration of CFD-derived heat transfer coefficients into a low-order dynamic model provides an effective compromise between computational efficiency and physical accuracy. This enables rapid evaluation of control strategies and makes the approach particularly suitable for both prototyping and embedded applications.

6. Conclusions

Based on the results and their critical interpretation, the final section summarizes the main contributions of the study and outlines future research directions.

This study presents a dynamic simulation model for an electric domestic oven, combined with an energy optimization strategy based on heating element control. The methodology integrates a steady-

state CFD analysis with a low-order dynamic model developed in MATLAB/Simulink, enabling accurate prediction of thermal behavior and energy consumption under standardized test conditions. Key findings include:

- The developed model demonstrated high accuracy in predicting the transient thermal evolution of the oven walls and cavity center. Temperature predictions for the cavity and walls showed an average error of less than 2% compared to experimental measurements.
- The energy analysis identified the grill and bottom heaters as the main contributors to convective and radiative heat losses, due to their high operating temperatures and specific placement.
- A multi-step control strategy was proposed to modulate the activation of the heating elements. This approach led to a significant reduction in energy consumption, with savings of up to 12.3%, without compromising the effectiveness of the cooking process.

The proposed modeling framework offers a valuable methodological contribution. By combining CFD-derived heat transfer coefficients with a lumped parameter dynamic model, it achieves a robust balance between physical fidelity and computational efficiency. This hybrid approach enables both accurate performance prediction and practical application in control-oriented design. It is particularly suited for fast prototyping, optimization studies, and potential real-time integration into embedded systems.

Future developments will focus on refining thermal load modeling and exploring advanced control strategies, such as model predictive control, to further improve energy efficiency and response precision.

Authors' contributions

Conceptualization, S.R., B.P., and M.R.; methodology, S.R.; software, S.R.; validation, S.R., B.P.; formal analysis, S.R.; investigation, S.R.; resources, B.P. and M.R.; data curation, S.R.; writing---original draft preparation, S.R.; writing---review and editing, S.R.; supervision, B.P., and M.R.; project administration, B.P.; funding acquisition, M.R. All authors have read and agreed to the published version of the manuscript.

Competing interests

The authors have no competing interests to declare.

Ethics and consent

All experimental procedures were conducted in accordance with industry standards and safety regulations. The oven used for testing is a commercially available, CE-marked domestic appliance compliant with applicable safety directives. The energy consumption tests followed the IEC 60350-1 standard for electric household cooking appliances. Data collection was performed in a controlled laboratory environment using calibrated instruments, in collaboration with the manufacturer's R&D department (SMEG), ensuring full compliance with ethical and technical best practices.

Acknowledgments

The authors would like to thank all SMEG employees who helped with the instruments during the tests in their workshops.

Fundings

This research received no external funding.

References

Amienyo D., J. Doyle, D. Gerola, G. Santacatterina, A. Azapagic, Sustainable manufacturing of consumer appliances: Reducing life cycle environmental impacts and costs of domestic ovens, Sust. Prod. Consum. 6 (2016) 67–76, https://doi.org/10.1016/j.spc.2015.12.004.

Åström, KJ & Hägglund, T 1995, *PID Controllers: Theory, Design, and Tuning*. ISA - The Instrumentation, Systems and Automation Society, Research Triangle Park, North Carolina.

Bansal P., E. Vineyard, O. Abdelaziz, Advances in household appliances- a review, Appl. Therm. Eng. 31 (2011) 3748–3760, https://doi.org/10.1016/j.applthermaleng.2011.07.023.

Burlon F., E. Tiberi, D. Micheli, R. Furlanetto, S. M, Transient model of a professional oven. {Energy Procedia} (2017), 126, 2–9, https://doi.org/10.1016/j.egypro.2017.08.045.

C.E. de Normalisation Electrotechnique (CENELEC), EN 60350-1 Household electric cooking appliances. Part 1: Ranges, ovens, steam ovens and grills Methods for measuring performance (latest version including all amendments), 2013.

Hoxha E., T. Jusselme, On the necessity of improving the environmental impacts of furniture and appliances in net-zero energy buildings, Sci. Total Environ. 596–597 (2017) 405–416, https://doi.org/10.1016/j.scitotenv.2017.03.107.

Lardeau, S.; Manceau, R. Computations of Complex Flow Configurations Using a Modified Elliptic-Blending Reynolds-Stress Model. In Proceedings of the 10th International ERCOFTAC Symposium on Engineering Turbulence Modelling and Measurements, Marbella, Spain, 17–19 September 2014.

Lauzier N. (Last accessed 26th January 2024). https://it.mathworks.com/matlabcentral/fileexchange/5664-view-factors?focused=5060891&tab=function

Lucchi M., Suzzi N., Lorenzini M., Dynamic model for convective heating of a wet brick during energy characterisation of domestic electric ovens. {Applied Thermal Engineering} (2019), 161, https://doi.org/10.1016/j.applthermaleng.2019.114117.

MATLAB \& Simulink https://www.mathworks.com/products/matlab-online.html

Mayil, Ayberk & Uğurelli, Can & Guzeltepe, Burak & Cengiz, Ayben. 2022 'Experimental study of electrical heater working function for improving energy consumption in a domestic oven'. In: ESKİŞEHİR TECHNICAL UNIVERSITY JOURNAL OF SCIENCE AND TECHNOLOGY A. {Applied Sciences and Engineering, Antalya, Turkey}

Mistry H., S. Ganapathisubbu, S. Dey, P. Bishnoi, J. Castillo, Modeling of transient natural convection heat transfer in electric ovens, Appl. Therm. Eng. 26 (2006) 2448–2456, doi: 10.1016/J.APPLTHERMALENG.2006.02.007.

Pensek, M & Holeček, Nikola & Gjerkeš, Henrik & Golobic, Iztok. (2005). Energy consumption analysis of domestic oven. Strojniski Vestnik/Journal of Mechanical Engineering. 51. 405-410, 10.1615/ICHMT.2004.IntThermSciSemin.560.

Ramirez-Laboreo E., C. Sagues, S. Llorente, Thermal modeling, analysis and control using an electrical analogy, in: 2014 22nd Mediterranean Conference on Control and Automation, MED 2014, pp. 505–510 (cited By: 4, 2014), 10.1109/MED.2014.6961423.

Edgar Ramirez-Laboreo, Carlos Sagues, Sergio Llorente, Dynamic heat and mass transfer model of an electric oven for energy analysis. {\em Applied Thermal Engineering} (2016), 93, 683-691, https://doi.org/10.1016/j.applthermaleng.2015.10.040.

Sari, Tamara & Celik, A. & Isik, O. & Temel, O. & Onbasioglu, Seyhan, 2013. 'Effects of insulation parameters on the energy consumption in domestic ovens and the most efficient insulation design'. At: EPJ Web of Conferences, 45, 01019, 10.1051/epjconf/20134501019.

Shaughnessy B.M, Newborough M, 2000 *'Energy performance of a low-emissivity electrically heated oven'*. Applied Thermal Engineering, Volume 20, Issue 9, Pages 813-830, https://doi.org/10.1016/S1359-4311(99)00072-1

Siegel, R.; Howell, J.R. Thermal Radiation Heat Transfer; Taylor & Francis: Washington, DC, USA, 1992, https://doi.org/10.1201/9780429327308.

Siemens Industries Digital Software. Simcenter STAR-CCM+ Academic Power on Demand. Available online: https://plm.sw.siemens.com/en-US/simcenter/fluids-thermal-simulation/star-ccm (accessed on 6 February 2024).

Verboven, P., Scheerlinck, N., De Baerdemaeker, J., Nicolaï, B.M., 2000a. Computational fluid dynamics modeling and validation of the temperature distribution in a forced convection oven. Journal of Food Engineering 43, 61–73, https://doi.org/10.1016/S0260-8774(99)00133-8.